Preprints, 10th IFAC International Symposium on
Advances in Automotive Control
Columbus, Ohio, USA, August 28-30, 2022

Modeling and Robust Coordinated Control of Turbocharged Natural Gas Engine with Genset Application

Weijin Qiu * **Sree Harsha Rayasam** * **Gregory M Shaver** *
Ted Rimstidt ** **Daniel G Van Alstine** ** **Michael Graziano** ***

* *Ray W. Herrick Laboratories, Mechanical Engineering, Purdue University, West Lafayette, IN 47907 USA (e-mail: qiu115@purdue.edu, srayasam@purdue.edu, and gshaver@purdue.edu).*
** *Caterpillar Inc., Lafayette, IN 47905 USA (e-mail: Rimstidt_Ted@cat.com, and Van_Alstine_Daniel_G@cat.com)*
*** *Caterpillar Inc., Mossville, IL 61552 USA (e-mail: Graziano_Michael_T@cat.com)*

Abstract: This paper describes a comprehensive framework for the development of a model-based robust coordinated control system, which is used to regulate the gas exchange processes of an advanced turbocharged natural gas engine with multifaceted control objectives. The natural gas engine involved in this study features a multi-input, multi-output structure and is highly-nonlinear. A robust coordinated control system is synthesized to realize desired performances of the engine over its entire operating region and is compared to a benchmark production control system in simulation. The comparison results explore the merits of coordinated control over decoupled control in the aspect of complex engine dynamics.

Keywords: Robust Control, Coordinated Control, Engine Control, Engine Modeling.

1. INTRODUCTION

Turbocharged natural gas engines have been widely used as power sources for stationary genset in recent years. However, harnessing their power efficiently through proper control of air handling management is indeed challenging for two main reasons. Firstly, the implementation of a turbocharger adds complexity and nonlinearity to the engine system, as well as interactions between each component involved in the engine.

Secondly, advanced turbocharged engine control problems are often multifaceted. One crucial control objective for an engine control system regulating such a kind of engine is being able to stabilize its engine speed so that the desired mains frequency could be provided regardless of disturbance load torque caused by varying electricity demands on the power grids. In addition to engine speed, the differential pressure across the engine throttle valve is also a key control objective to be considered for avoiding compressor surge, which could potentially damage the turbocharger. Apart from engine speed and throttle differential pressure, air-to-fuel ratio (AFR) is extremely critical as well. Engine performances in terms of fuel consumption and NOx emissions are highly dependent on AFR, and the fact that natural gas engines are expected to be operated near the lean burn limit puts forward the demand for controlling AFR precisely and promptly.

There have been several pieces of research aimed at addressing engine control problems by exploiting robust control theory. Dolovai et al. (2008) proposed a robust H_∞ controller for speed control of a natural gas engine with fairly good performance over the entire operating region of the engine. Zope et al. (2010) designed a gain-scheduled H_∞ controller to regulate AFR for an SI engine over a large operating region. However, there are not many studies revealing the merits of robust coordinated control on engine control problems where the interactions between multiple actuators and multiple control objectives are handled simultaneously and jointly. This work presents a comprehensive framework for synthesizing a robust coordinated control system to solve multifaceted engine control problems arising from engine performance requirements, safe operation, and emission regulation.

This paper is organized as follows. After the introduction in Section 1, a control-oriented mathematical model for the engine is developed and validated against a truth-reference GT-Power [1] engine model in Section 2. The procedure of synthesizing a robust coordinated control system based on the model developed previously is presented in Section 3. In Section 4, the performance of the synthesized robust control system is examined and compared to a benchmark production control system developed by the engine manufacturer Caterpillar. Finally, Section 5 draws the main conclusions in conjunction with the contributions of this study. Suggestions for future work are also provided.

⋆ The authors disclosed receipt of the following financial support for the research, authorship, and publication of this artical: This effort was funded by Caterpillar Inc.

[1] GT-Power is a registered trademark of Gamma Technologies, LLC.

2. CONTROL-ORIENTED ENGINE MODELING

2.1 Engine Architecture

The engine architecture is depicted in Fig. 1 and the arrows at various points represent the direction of gas flow under normal operating conditions. This engine system features three actuators: throttle valve, bypass valve, and fuel valve. Noted that there is a passive wastegate valve. The control outputs are engine rotational speed, the differential pressure across the throttle valve (as a means to prevent compressor surge), and AFR (to restrict engine emissions).

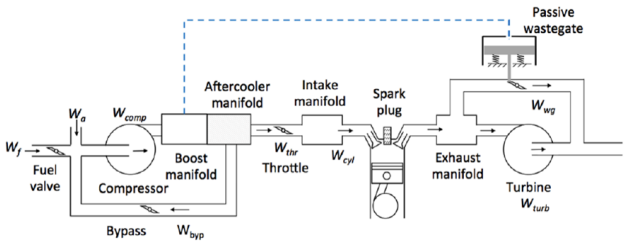

Fig. 1. Engine architecture

2.2 Engine Modeling

The control-oriented model would be represented in state-space form, which consists of five state variables, three input variables, one disturbance variable, and three output variables. Table 1 summarizes the definition of all these variables with explicit indication and unit.

Table 1. Control-oriented model variables

Variable	Description	Unit
State (x_1)	Engine speed	rad/s
State (x_2)	Intake manifold pressure	Pa
State (x_3)	Compressor manifold pressure	Pa
State (x_4)	Exhaust manifold pressure	Pa
State (x_5)	Turbocharger speed	rad/s
Input (u_1)	Effective throttle area	m^2
Input (u_2)	Effective bypass area	m^2
Input (u_3)	Fuel flow rate	kg/s
Disturbance (d)	Load torque	Nm
Output (y_1)	Engine speed	rad/s
Output (y_2)	Differential pressure across throttle valve	Pa
Output (y_3)	AFR	-

Based on the conservation laws of mass and energy in Heywood (2018), the nonlinear mathematical model of the studied engine can be obtained and expressed as shown below.

$$\begin{aligned}
\dot{x_1} &= \frac{1}{I_{eng}}\left[\frac{\eta_v \eta_{therm} Q_{lhv} V_d u_3}{4\pi R T_{im} W_{cyl}} x_2 - d\right] \\
\dot{x_2} &= \frac{RT_{im}}{V_{im}}[W_{thr} - W_{cyl}] \\
\dot{x_3} &= \frac{RT_{bm}}{V_{bm}}[W_{comp} - W_{thr} - W_{byp}] \\
\dot{x_4} &= \frac{RT_{em}}{V_{em}}[W_{cyl} - W_{turb} - W_{wg}] \\
\dot{x_5} &= \frac{P_{turb} - P_{comp}}{I_{tc} x_5}
\end{aligned} \tag{1}$$

Multiple terms involved in the nonlinear model are treated as constants, namely: engine shaft inertia I_{eng}, volumetric efficiency η_v, lower heating value of the fuel Q_{lhv}, engine displacement V_d, gas constant R, turbocharger shaft inertia I_{tc}, temperature T and the volume V of each manifold.

Terms that can't be treated as constants are modeled as functions of state variables and/or input variables, see Table 2. For their explicit expressions and physics-based derivations, please refer to Harsha Rayasam et al. (2021).

Table 2. Summary of necessary sub-models

Term	Description	Strategy
η_{therm}	Thermal efficiency	$fcn(y_3)$
W_{cyl}	Cylinder mass flow	$fcn(x_1, x_2)$
W_{thr}	Throttle mass flow	$fcn(u_1, x_2, x_3)$
W_{byp}	Bypass mass flow	$fcn(u_2, x_3)$
W_{wg}	Wastegate mass flow	$fcn(x_4)$
W_{comp}	Compressor mass flow	$fcn(x_3, x_5)$
W_{turb}	Turbine mass flow	$fcn(x_4, x_5)$
P_{comp}	Compressor power	$fcn(x_3, x_5)$
P_{turb}	Turbine power	$fcn(x_4, x_5)$

Once the nonlinear mathematical model is obtained, it can be linearized around an equilibrium point to get a linear, control-oriented, physics-based model expressed in standard state-space form as follows.

$$\begin{aligned}
\dot{x} &= Ax + Bu + Vd \\
y &= Cx + Du
\end{aligned} \tag{2}$$

2.3 Model Validation

To validate the proposed nonlinear and linear model, an open-loop validation strategy incorporating a benchmark production control system and a high-fidelity GT-Power engine model developed by Caterpillar is adopted. This GT-Power model has been calibrated against a real lab engine with high accuracy and therefore is regarded as the truth-reference model in this study. The benchmark control system regulates the performances of the GT-Power engine model through closed-loop control under different load torque conditions in simulation. The control inputs commanded by the control system are extracted along with disturbance and sent into the nonlinear/linear model. The engine outputs predicted by the mathematical models can then be compared to the engine outputs from the GT-Power model. The essential idea behind this validation approach is that models with the same dynamics should respond to the same inputs and disturbance identically. Fig. 2 illustrates this open-loop strategy.

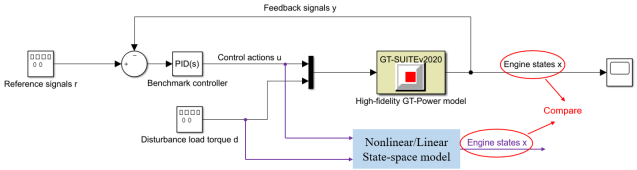

Fig. 2. Illustration of validation strategy

The validation results are shown in Fig. 3. It can be observed that the nonlinear model matches well with the truth-reference GT-Power model, as there is no obvious deviation between the two model data over the entire

operating region. On the other hand, there exist some deviations between the linear model and the truth-reference model, which complies with the fact that loss of model fidelity and accuracy could occur in the regions away from the equilibrium point, which in this case is the operating condition at 60% of the engine rated power.

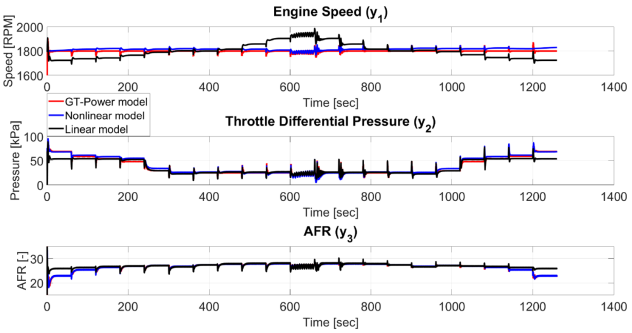

Fig. 3. Validation result for nonlinear/linear model

3. ROBUST COORDINATED CONTROLLER DESIGN

3.1 Formation of Perturbed Model

To design a coordinated controller out of a less accurate linear model, a perturbed-model approach illustrated in Fig. 4 is considered in this study. This approach incorporates perturbations/uncertainties into the linear model to obtain a perturbed linear model, whose dynamics should cover the dynamics of the studied engine. Then a robust coordinated controller can be synthesized which should stabilize the perturbed linear model, and as a natural result, should also stabilize the engine system.

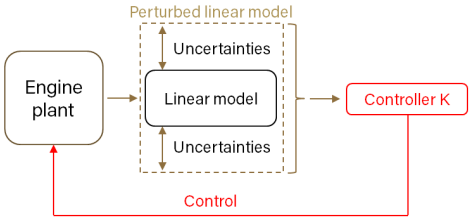

Fig. 4. Illustration of perturbed-model approach

Denote the nominal linear model as G_o and the perturbed model as G_p. An output multiplicative perturbation used to link the two models per Gu et al. (2005) is formed in 3, where k_i and τ_i indicate the pre-specified gain and phase variation in the i_{th} output channel, respectively.

$$G_p(s) = W_{unc}G_o(s) = \begin{bmatrix} k_1 e^{-\tau_1 s} & 0 & 0 \\ 0 & k_2 e^{-\tau_2 s} & 0 \\ 0 & 0 & k_3 e^{-\tau_3 s} \end{bmatrix} G_o(s) \tag{3}$$

By setting perturbation block $\|\Delta_i\|_\infty < 1$, representing W_{unc} in terms of uncertainty weighting function W_Δ yields

$$W_{unc} = I + W_\Delta \Delta = I + \begin{bmatrix} W_{\Delta_1} & 0 & 0 \\ 0 & W_{\Delta_2} & 0 \\ 0 & 0 & W_{\Delta_3} \end{bmatrix} \begin{bmatrix} \Delta_1 & 0 & 0 \\ 0 & \Delta_2 & 0 \\ 0 & 0 & \Delta_3 \end{bmatrix} \tag{4}$$

Denoting the nominal transfer function in the $i_{th}(i = 1, 2, 3)$ output channel ($k_i = 1, \tau_i = 0$) by $\overline{W}_{unc_i}$ and taking into account that $\|\Delta_i\|_\infty < 1$ yields the following

$$\left\| \frac{W_{unc_i}(j\omega) - \overline{W}_{unc_i}(j\omega)}{\overline{W}_{unc_i}(j\omega)} \right\|_\infty \leq \|W_{\Delta_i}(j\omega)\|_\infty, \forall \omega \in \mathbf{R} \tag{5}$$

That is, to choose the uncertainty weighting function W_{Δ_i} is equivalent to determining an upper bound of the relative uncertainty on the left side of 5 in terms of H_∞-norm. Applying Euler's formula yields

$$\sqrt{([k_i cos(\omega\tau_i) - 1]^2 + [k_i sin(\omega\tau_i)]^2)} \leq \|W_{\Delta_i}(j\omega)\|_\infty, \forall \omega \in \mathbf{R} \tag{6}$$

The magnitude of the term on the left of 6 can be easily calculated at any frequency for specific k_i and τ_i. Designing a transfer function whose frequency response is greater than that of all the possible uncertainties within the pre-specified k_i and τ_i range at all frequencies yields the uncertainty weighting function for i_{th} output channel W_{Δ_i}. Fig. 5 demonstrates uncertainty modeling for the three control outputs in this study: engine speed, throttle differential pressure, and AFR.

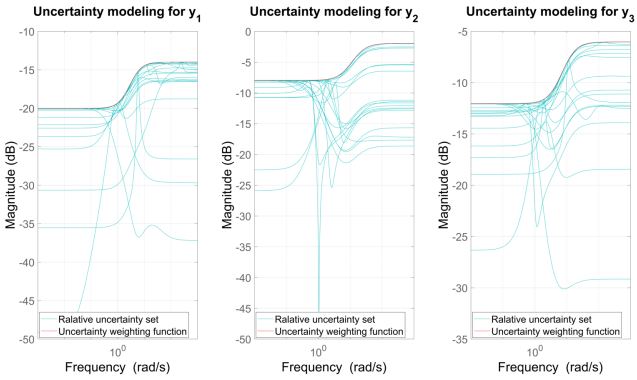

Fig. 5. Output multiplicative uncertainty modeling

With the efforts described above, a perturbed model has been obtained, based on which a robust coordinated controller can be synthesized as shown in the next subsection.

3.2 Controller Synthesis

Fig. 6 presents the block diagram of the proposed control system intending to formulate the control problem explicitly and accurately.

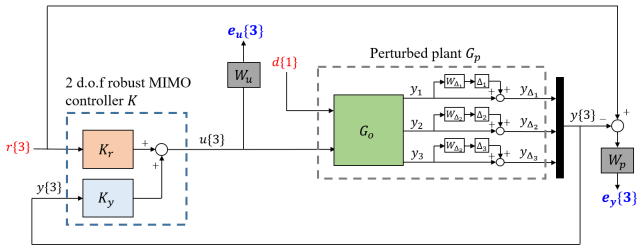

Fig. 6. Control block diagram

The proposed control system features a two-degree-of-freedom robust coordinated controller $K = [K_r \ K_y]$ where

three reference signals r (target engine speed, target throttle differential pressure, and target AFR) go through the feedforward path K_r and three measured outputs y (actual engine speed, actual throttle differential pressure, and actual AFR) go through the feedback path K_y. The controller would command appropriate control actions u to the perturbed engine plant G_p to counteract the effect of disturbance load torque d. To penalize nonzero tracking errors and excessive actuator efforts, two transfer function matrices, namely performance weighting function matrix W_p and control weighting function matrix W_u, are artificially set up to obtain weighted performance errors e_y and weighted actuator efforts e_u, which can be recast as *exogenous outputs* of the proposed control system. On the flip side, the reference signals r and disturbance input d act as *exogenous inputs*. The essential goal of robust coordinated control design is to minimize the exogenous outputs regardless of the exogenous inputs.

To formulate the control problem mathematically, splitting the perturbed plant into two parts $G_p = [G_u \; G_d]$ such that $y = G_u u + G_d d$, then the transfer function matrix from exogenous inputs to exogenous outputs in the Laplace domain can be worked out as

$$\begin{bmatrix} e_y \\ e_u \end{bmatrix} = \underbrace{\begin{bmatrix} W_p\left(\left(I+G_uK_y\right)^{-1}G_uK_r - I\right) & W_p\left(I+G_uK_y\right)^{-1}G_d \\ W_u\left(I+K_yG_u\right)^{-1}K_r & -W_u\left(I+K_yG_u\right)^{-1}K_yG_d \end{bmatrix}}_{M(G_p,K)} \begin{bmatrix} r \\ d \end{bmatrix} \tag{7}$$

Robust control theory covered in Skogestad and Postlethwaite (2007) specifies that to synthesize a robust coordinated controller which ensures robust stability and robust performance of the interconnected system $M(G_p, K)$, the following inequality needs to be satisfied

$$\sup_{\omega \in \mathbf{R}} \mu_{\Delta}\left[M(G_p,K)\right](j\omega) < 1 \tag{8}$$

The above expression formulates the control problem mathematically. To synthesize such a controller K, the μ-synthesis method by D-K iteration using MATLAB [2] is adopted, which iteratively solves a convex optimization problem involving controller K until a feasible controller K is obtained.

Synthesizing a robust coordinated controller requires extensive and iterative tuning on each of the performance weighting functions, as the shaping of performance weighting functions significantly determines the resultant closed-loop control system performances by affecting controller synthesis in terms of adjusting the expression of the interconnected system $M(G_p, K)$. However, not much work has been performed on finding reliable methods of selecting appropriate performance weighting functions. Therefore, a generalizable tuning guide proved to work fairly well in this study is developed and presented in Fig. 7. It should be noted that this tuning guide provides only some modest insights into the selection of performance weighting functions, and is not the only method for robust coordinated controller tuning.

[2] MATLAB is a registered trademark of The MathWorks, Inc.

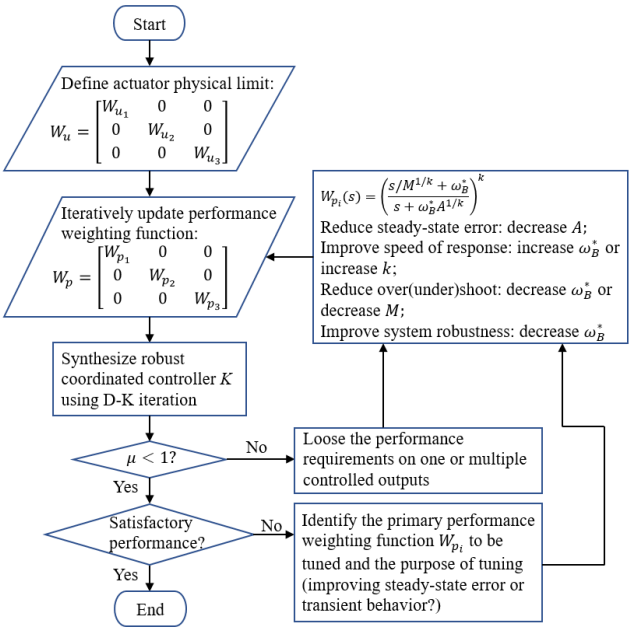

Fig. 7. Generalizable tuning guide

3.3 Properties of Synthesized Control System

Fig. 8 presents the inverse of the performance weighting function selected for each control output, which possesses a deterministic impact on the properties and performances of the resultant control system synthesized in this study.

Comparing the magnitude of three performance weighting functions' inverse at lower frequency indicates that there should be very little tracking error at steady state for engine speed and AFR, while one should expect some steady-state error for throttle differential pressure.

On the other hand, at the higher frequency, it can be expected that there would exist more over(under)shoot in throttle differential pressure, as its performance weighting function's inverse has greater value in this region. What's more, the inverse of the performance weighting function for engine speed and AFR are more rightward on the Bode plot, indicating that their transient response would be faster than that of throttle differential pressure. In short, fairly good control should be observed for engine speed and AFR, while slightly worse transient response and steady-state error would be observed for throttle differential pressure. The selection of presented performance weighting functions takes into consideration of performance requirements on the resultant control system set up by the engine manufacturer, as well as necessary robustness requirements to ensure system stability against disturbance and model variation.

The control weighting functions for control inputs are selected based on the actual physical limits of engine actuators and omitted in this paper for simplicity. Briefly summarizing, with the aid of the μ-synthesis, a 22nd order controller is synthesized for which the peak μ value is obtained at 0.875 thus achieving closed-loop robust stability and robust performance in theory.

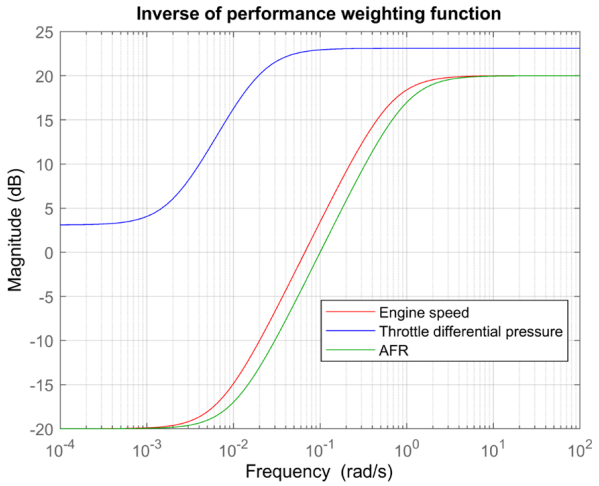

Fig. 8. Performance weighting functions

4. SIMULATION AND ANALYSIS

This section examines the performances of the robust coordinated control system synthesized in this study. A benchmark production control system composed of multiple single input single output (SISO) gain-scheduled PID controllers developed by Caterpillar is deployed for running the same simulation. Both control systems are implemented on the same truth-reference GT-Power, and the simulation results obtained using two different control systems would be compared and analyzed.

4.1 Simulation Drive Cycle Profile

The drive cycle profile realized in simulation for controller testing is briefly described here. In terms of disturbance, the load torque undergoes a step-change equivalent to 25% of maximum load every sixty seconds, starting from 0 to 100%, and then back down to 0. This load profile is a typical test maneuver performed by Caterpillar, featuring aggressive load torque change imposed on the engine, which emulates significant and sudden variation of electricity demands on the power grid. In terms of three control outputs, the target engine speed is fixed at a constant 1800 RPM for 60Hz output frequency, while the target throttle differential pressure and target AFR are obtained using the lookup tables provided by Caterpillar, which are dependent on actual engine speed and actual load torque.

4.2 Simulation Results and Analysis

Fig. 9 presents simulation results of engine speed regulated by the two control systems. Note that the pink lines mark the region within which engine speed should stay at a steady state. Fig. 10 provides several exploded views of this simulation. It can be observed that the robust coordinated controller yields better transient response over the entire operating region in engine speed, featuring less recovery time and speed droop. In addition to the fact that the benchmark control system is unable to stabilize engine speed at the highest load highlighted by continuous oscillation between 250 and 300 seconds, the benchmark control system also struggles with recovering engine speed through the course of load reduced from 100% to 75%, as much more significant undershoot is observed.

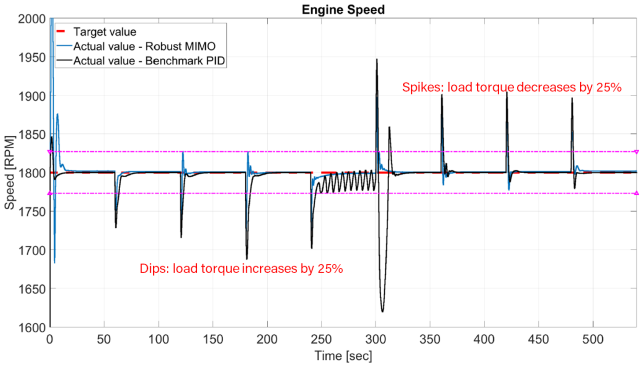

Fig. 9. Simulation result - engine speed (control output)

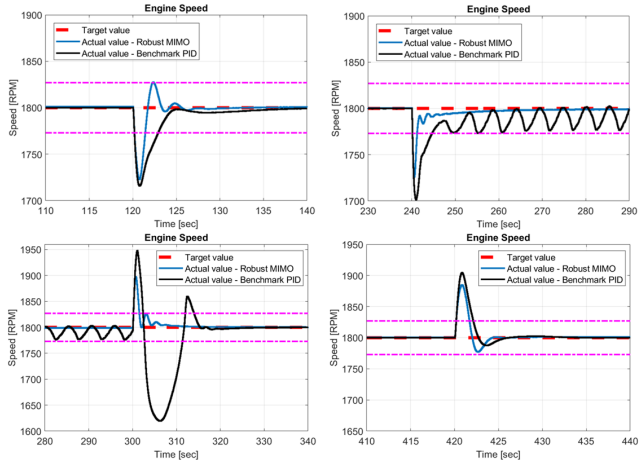

Fig. 10. Exploded views - engine speed (control output)

Similar observation can be made as well for AFR response per Fig. 12. Better tracking of AFR is achieved by the robust coordinated control system over the entire operating region, featuring smaller steady-state tracking errors and faster response.

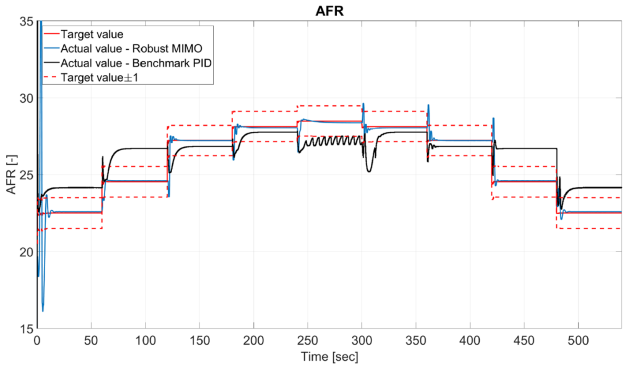

Fig. 11. Simulation result - AFR (control output)

As shown in Fig. 12, at low load conditions, better tracking of throttle differential pressure is achieved by the robust coordinated controller. However, at the highest load condition, better tracking of throttle differential pressure is observed with the benchmark control system. Be reminded that the tracking of throttle differential pressure is to prevent compressor surge. After checking the compressor map, it is confirmed that there is no compressor surge in either of the two cases.

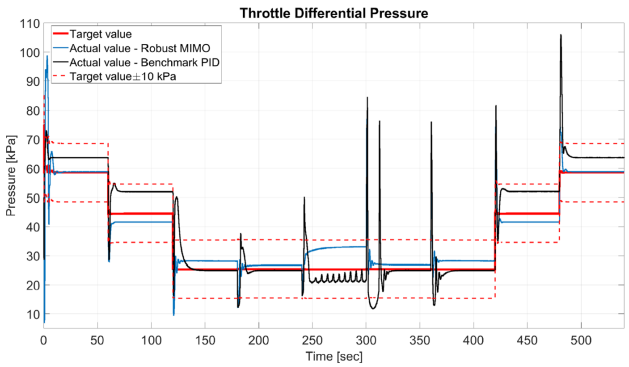

Fig. 12. Simulation result - throttle differential pressure (control output)

In Fig. 13, the three control actions commanded by the two different control systems and one same disturbance load torque are presented. Due to confidentiality, the actual values of these measurements are scaled concerning their maximum magnitude.

It can be observed that the most significant variation between the two control systems lies in the bypass valve actuation commands. At the highest load torque condition, the benchmark control system actuates the bypass valve to a greater extent. Recall that the bypass valve is used to release boost pressure when the compressor is inducting too much air, this valve actuation by the benchmark control system leads to the release of more boost pressure and as a result lower throttle differential pressure which is good if throttle differential pressure is the only control output. However, the more actuated bypass valve commanded by the benchmark controller restricts the capability of the compressor to draw more air into the engine. Without enough air, the engine speed can't be maintained at 1800 RPM, as reflected in Fig. 9 from 250 to 300 second. Therefore, the benchmark control system tries to fully open the throttle valve to provide the engine with more air but fails eventually.

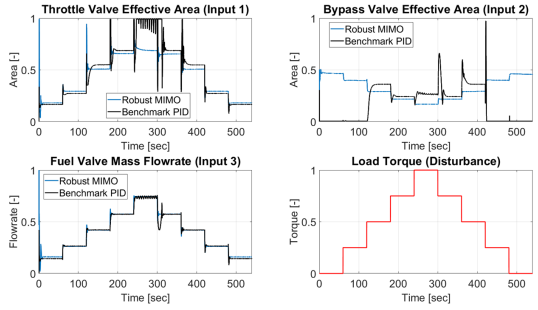

Fig. 13. Simulation result - control inputs and disturbance

The above discussions reveal one of the most important benefits of utilizing a coordinated control system: better coordination between different actuator control actions. When the benchmark control system is working, each one of the multiple internal SISO controllers targets its own individual control objective only, which sometimes leads to a scenario where the performance of one controlled output of greater importance is sacrificed for the performance of another controlled output of less importance. This issue can be resolved using a coordinated control system as the level of importance for different control objectives can be specifically indicated during the controller design process, and the resultant control commands would be generated in accordance with this layout. In another word, actuation commands are generated in a manner that would satisfy a certain hierarchy of priority in terms of controlled output, which is arranged through an appropriate selection of performance weighting functions.

5. CONCLUSION

Multifaceted control problems are often inherent in advanced turbocharged engines, for which a coordinated control system could be an ideal solution. This paper outlines a comprehensive framework for the development of such a control system.

To synthesize a model-based robust coordinated control system, a physics-based, control-oriented mathematical model is developed and validated first. A generalizable procedure for the synthesis of a robust coordinated control system is then presented, including uncertainty modeling, formulation of controller synthesis, and controller tuning. To test the performances of the synthesized robust coordinated control system, a direct comparison between the benchmark production control system developed by Caterpillar and the robust coordinated control system is achieved by implementing both control systems on a truth-reference high-fidelity GT-Power engine model and performing the simulation under the same conditions. Through those comparisons, the merit of applying coordinated control is realized.

For future research efforts, it is suggested that controller-order reduction be realized, as the current controller of 22nd-order tends to cause high cost, difficult commissioning, and potential problems in maintenance. Apart from that, experiments of implementing the synthesized robust coordinated controller on a test bench engine should be conducted if the opportunity arises.

REFERENCES

Dolovai, P., Joergl, H., and Hirzinger, J. (2008). H_∞ controller design for speed control of a natural gas engine. In *2008 27th Chinese Control Conference*, 642–647. IEEE.

Gu, D.W., Petkov, P., and Konstantinov, M.M. (2005). *Robust control design with MATLAB®*. Springer Science & Business Media.

Harsha Rayasam, S., Qiu, W., Rimstidt, T., Shaver, G.M., Van Alstine, D.G., and Graziano, M. (2021). Control-oriented modeling, validation, and interaction analysis of turbocharged lean-burn natural gas variable speed engine. *International Journal of Engine Research*, 14680874211064210.

Heywood, J.B. (2018). *Internal combustion engine fundamentals*. McGraw-Hill Education.

Skogestad, S. and Postlethwaite, I. (2007). *Multivariable feedback control: analysis and design*, volume 2. Citeseer.

Zope, R., Mohammadpour, J., Grigoriadis, K., and Franchek, M. (2010). Robust fueling strategy for an si engine modeled as an linear parameter varying time-delayed system. In *Proceedings of the 2010 American Control Conference*, 4634–4639. IEEE.